Cerrahpaşa Med J 2021; 45(3): 197-204 ORIGINAL ARTICLE / ÖZGÜN ARAŞTIRMA

Evaluation of the Extension of Benign and Malignant Microcalcifications by Breast Magnetic Resonance Imaging, Mammography, and Ultrasonography

Deniz Esin Tekcan Şanlı[1,2], Yasemin Kayadibi[3], Neşe Uçar Yiğitoğlu[4], Emel Esmerer[5], Mustafa Tarık Alay[6], Ahmet Necati Şanlı[7]

[1]Department of Medical Imaging Techniques, Vocational School of Health Services, İstanbul Rumeli University, İstanbul, Turkey
[2]Department of Radiology, Acıbadem Kozyatağı Hospital, İstanbul, Turkey
[3]Department of Radiology, İstanbul University-Cerrahpaşa, Cerrahpaşa School of Medicine, İstanbul, Turkey
[4]Department of Radiology, İstanbul Gaziosmanpaşa Training and Research Hospital, İstanbul, Turkey
[5]Department of Radiology, İstanbul Esenler Gynecology and Pediatrics Hospital, İstanbul, Turkey
[6]Department of Medical Genetics, İstanbul University-Cerrahpaşa, Cerrahpaşa School of Medicine, İstanbul, Turkey
[7]Department of General Surgery, İstanbul University-Cerrahpaşa, Cerrahpaşa School of Medicine, İstanbul, Turkey

Cite this article as: Esin Tekcan Şanlı D, Kayadibi Y, Uçar Yiğitoğlu N, Esmerer E, Tarık Alay M, Necati Şanlı A. Evaluation of the extension of benign and malignant microcalcifications by breast MRI, mammography and ultrasonography. *Cerrahpaşa Med J.* 2021;45(3):197-204.

Abstract

Objective: The aim of this study was to compare the mammographic microcalcification areas with pathological enhancement in magnetic resonance imaging and heterogeneous areas in ultrasonography.

Methods: Patients with microcalcification evaluated in the category of Breast Imaging Reporting and Data System (BI-RADS) 4-5 mammographically were examined by both ultrasonography and contrast-enhanced breast magnetic resonance imaging. The morphological type of microcalcifications by mammography, distribution pattern, and total distribution area were evaluated. The related imaging features with ultrasonography and distribution areas were evaluated. The area of the contrast-enhanced tissue, its distribution, enhancement kinetics (types 1, 2, and 3), and diffusion restriction were evaluated by magnetic resonance imaging. The widest dimensions of the pathological areas detected in all 3 examinations were statistically compared.

Results: A total of 42 cases were included in the study. Although the most common mammographic microcalcification pattern in both groups was pleomorphic, it was significantly higher in the malignant group ($P = .037$). According to histopathological subtypes, the largest pathological area was seen in the invasive lobular carcinoma and invasive ductal carcinoma accompanying with ductal carcinoma in situ. Although the sizes of malignant lesions on magnetic resonance imaging and ultrasonography were larger than benign ones, no significant difference was found ($P > .05$). There was a statistically significant moderate correlation between mammography and ultrasonography in showing both benign and malignant lesions, but no correlation was observed with magnetic resonance imaging (in benign lesions ($P = 0.658$, $P = .004$; in malignant lesions $P = 0.519$, $P = .008$).

Conclusion: Contrast enhancement may not be seen with magnetic resonance imaging in low-grade or early-onset ductal carcinoma in situ cases; therefore, in the presence of suspicious sonomammographic findings, even if magnetic resonance imaging examination is negative, further histological evaluation should be performed.

Keywords: Malignant microcalcification, DCIS, breast MRI, invasive ductal carcinoma, mammography

Benign ve Malign Mikrokalsifikasyonların Meme MR, Mamografi ve Ultrasonografi İle Yayılımının Değerlendirilmesi

Öz

Amaç: Mamografik mikrokalsifikasyonların benign ve malign olma durumuna göre mamografik dağılım alanları ile, manyetik rezonans incelemede (MR) patolojik kontrastlanma ve ultrasonografi (US) de heterojenite yayılımlarını karşılaştırmak

Received: May 4, 2021 **Accepted:** September 14, 2021 **Available Online Date:** November 7, 2021
Corresponding author: Deniz Esin Tekcan Şanlı, Department of Medical Imaging Techniques, Vocational School of Health Services, İstanbul Rumeli University, İstanbul, Turkey
e-mail: tekcandenizesin@gmail.com
DOI: 10.5152/cjm.2021.21041

Yöntemler: Mamografik olarak BIRADS 3-4-5 kategorisindeki mikrokalsifikasyonlar MR ve US ile değerlendirildi. Mmg'de mikrokalsifikasyonların morfolojik tipi, dağılım paterni ve alanı; US'de bu mikrokalsifikasyonlarla ilişkili özellikler (ekojenik fokus, mikrokist kümesi, duktal ektazi, heterojenite, hipoekojenite) ve alanı, MR'da patolojik kontrastlanma dağılımı, kinetiği ve difüzyon kısıtlanması değerlendirildi. Her üç incelemede kaydedilen patolojik alan boyutları istatiksel olarak karşılaştırıldı.

Bulgular: Çalışmaya 42 hasta dahil edildi. Benign olguların yaş ortalaması (s:17) 44,17 ± 7,56; malign olguların ise (s:25) 44,64 ± 11,32 olup anlamlı farklılık saptanmadı ($P < ,05$). Her iki grupta en sık görülen mikrokalsifikasyon tipi pleomorfik olmakla birlikte malign grupta anlamlı olarak daha yüksekti (P: ,037). Histopatolojik subtiplere göre en geniş patolojik alan boyutu invaziv lobuler karsinom ile invaziv lobuler karsinom + duktal karsinoma insitu bileşenlerinde saptandı. Malign alanların MR ve US boyutları benignlerden yüksek olmakla birlikte anlamlı farklılık saptanmadı ($P > ,05$). Benign ve malign lezyonları göstermede Mmg ve US korele olmakla birlikte MR ile korelasyon saptanmadı (benign $P = ,658$, $P = ,004$; malign: $P = 0.519$, $P = ,008$).

Sonuç: Düşük dereceli veya erken başlangıçlı DCIS olgularında MR ile patolojik kontrastlanma görülmeyebilir, bu nedenle şüpheli sonomamografik bulguların varlığında MR incelemesi negatif olsa bile ileri histolojik değerlendirme yapılmalıdır.

Anahtar Kelimeler: Malign mikrokalsifikasyon, DKIS, meme MR, invaziv duktal karsinom, mamografi

The diagnosis of ductal carcinoma in situ (DCIS), which is accepted as a precursor of invasive breast cancer, has significantly increased with the widespread use of screening mammographies.[1] Although most of the calcifications that can be detected mammographically are benign microcalcifications, the most common mammographic finding of DCIS is microcalcifications.[1] The predictive value of microcalcifications in terms of malignancy according to their morphology and distribution pattern has been frequently discussed in literature studies up to now; fine linear, fine pleomorphic, or branching microcalcifications with linear and segmental distribution are the most associated calcifications with malignancy (Table 1, Figures 1 and 2).[1,2]

Although mammography (MMG) plays an important role in detecting microcalcification and contributes greatly to the detection of breast cancer at an early stage, it gives limited information about the actual extension of the disease.

Table 1. Classification of Mammographic Calcifications According to BI-RADS Categories

Calcification Type	Category
Skin calcifications	BI-RADS 2
Milk of calcium calcifications	
Thick linear calcifications	
Popcorn calcifications	
Dystrophic calcifications	
Round, scattered, or isolated calcifications	
Vascular calcifications	
Suture calcifications	
Round grouped calcifications	BI-RADS 3
Coarse, rough, heterogeneous calcifications	BI-RADS 4B
Amorphous calcifications	
Fine pleomorphic calcifications	
Linear or branched linear calcifications	BI-RADS 4C
Linear and new branching linear and segmental distribution calcifications	BI-RADS 5

Recently, although there are various studies proving that contrast-enhanced MMG can be used in these indications, it could not reach the expected prevalence due to radiation exposure and use of iodinated contrast material.[3] In addition to evaluating the extension of the disease, the most frequently used and most sensitive method is contrast-enhanced dynamic breast magnetic resonance imaging (MRI) to determine the preoperative local staging and treatment method of the disease by evaluating the condition of the contralateral breast and axilla.[4] In this study, MMG, US and MRI findings of histopathologically proven microcalcifications classified as BI-RADS 4-5 in MGM were compared. The advantages and disadvantages of these three methods were discussed in the light of the literature.

Methods

Study population

Patients above the age of 40 who underwent MMG due to routine breast screening or who under the age of 40 underwent MMG after US due to palpable lesion complaints and family history in our hospital between April 2019 and January 2021 were evaluated. Patients with histopathologically proven microcalcification in the category BI-RADS 3-4-5 in MMG and showed contrast enhancement without mass formation with MRI were included in the study. Signed informed consent forms were obtained from all patients before MMG. Ethics committee approval was obtained from the institution that our hospital is affiliated with for the study (April 14, 2021, 252). Patients with a history of breast surgery for any reason and a diagnosis of known breast cancer were excluded from the study.

Imaging method and image analysis

All mammographic examinations were performed in standardized mediolateral oblique and craniocaudal positions (Giotto Image MC, IMS, Italy). According to ACR-BI-RADS 5th edition (2013), mammographic breast density (types A, B, C, and D), microcalcification type (amorphous, fine pleomorphic, coarse heterogeneous, fine linear and fine linear branching) (Figure 1), distribution pattern (clustered, regional, segmental, diffuse, linear) (Figure 2), and BI-RADS category (4A, 4B, 4C, 5) of the patients were evaluated.[5] Microcalcifications without mass in MMG lesions were included in the study. The widest microcalcification

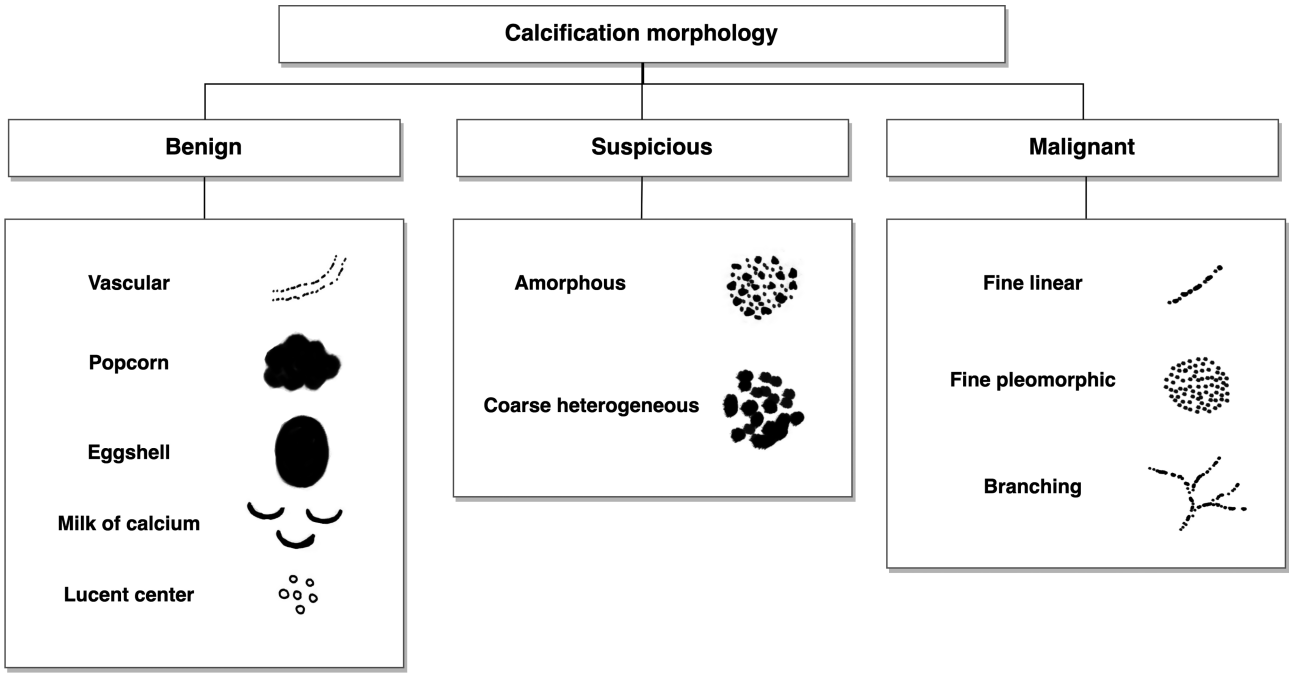

Figure 1. Morphological classification of mammographic microcalcifications according to malignancy suspicion.

distribution area (mm^2) was examined with other findings (asymmetric density increase, parenchymal distortion) accompanying microcalcifications on MMG.

Later, these patients underwent US. All sonographic examinations were performed on the Toshiba Aplio 500 software version 6.0 (Toshiba Corporation, Tokyo, Japan). Ultrasonographic accompanying changes associated with microcalcifications (echogenic focus with US) (hypoechoic area, irregularly dilated ducts, microcyst cluster, parenchymal distortion) were evaluated. The sonographic widest dimensions of these echogenic foci and other associated findings were measured.

All patients underwent contrast-enhanced breast MRI due to suspicion of malignancy. All MRI examinations were performed with a 1.5 Tesla MRI equipment (GE Signa HDx, GE Medical Systems, USA) using an 8-channel phased-array breast surface coil. All breast MRI exams were performed on the 7th-15th day of the menstrual cycle of patients. The settings of the conventional contrast-enhanced MRI were fat-suppressed 3D T1-weighted images (4.3 ms/1.4 ms; flip angle, 12°; an Field-of-view (FOV) of 320 mm; matrix, 307 × 512; signal average 1; slice thickness, 1.5 mm fast low-angle shot) with 1 acquisition before contrast injection and acquisitions up to 6 minutes after. The contrast agent (Dotarem, Laboratoire Guerbet, Roissy, France) was administered as 0.2 mmol/kg by using mechanical power injector, followed by 15-20 cc of saline. Properties of the axial diffusion-weighted echo-planar images were repetition time (TR) / echo time (TE) 8500/70, FOV of 330 mm, matrix 192 × 192, NEX 1, sectional thickness 4.5 mm with a 1-mm intersection gap with diffusion gradients between 0 and 1000 sec/mm^2 b values. Breast MRI was evaluated in terms of widest enhancement area (mm^2), distribution pattern (focal, linear, segmental, regional, diffuse), enhancement kinetics (type 1 (persistent enhancement), type 2 (plateau-style enhancement), type 3 (wash-out)), and whether it showed diffusion restriction. All images were evaluated together by 2 radiologists (N.U, Y.K.) experienced in breast radiology.

Biopsy technique

Microcalcifications detected only by MMG were sent to surgical excision after mammographically guided wire localization. Sampling of mammographic microcalcifications which were detected by US was performed as core biopsy with a 16-gauge needle under local anesthesia with US. No biopsy was performed under MRI. To be at least 7, an average of 10 samples were taken from each lesion. After the biopsies, the specimen graphies were taken, and it was checked whether it contained calcification. If not, the biopsy procedures were

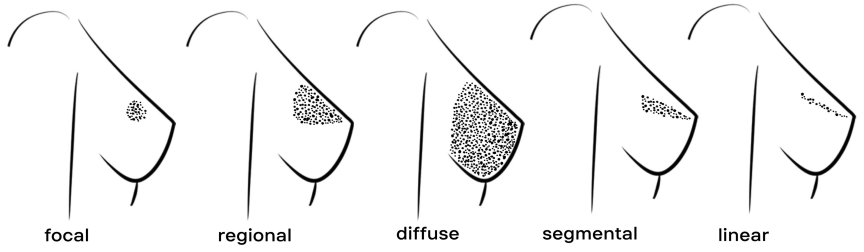

Figure 2. Schematic representation of mammographic microcalcifications according to distribution.

repeated. All biopsy procedures were performed under sterile conditions, and the samples taken were sent to the pathology laboratory in sterile boxes.

Histopathological evaluation

The histological type and grade of the samples (according to the Scarff-Bloom-Richardson grading system), estrogen receptor, progesterone receptor status, and human epidermal growth factor receptor (Her2) positivity were examined.

Statistical analysis

While numbers and percentages were used for categorical data in the measurement of descriptive statistics, mean and standard deviation were used when appropriate for normal distribution in the measurement of numerical data, while minimum, maximum, and median were used in the measurement of data that were not suitable for normal distribution. Student's *t* test, analysis of variance, Mann–Whitney U, Kruskal–Wallis, and chi-square tests were used as basic statistical methods. In cases where the chi-square method could not be applied, Yates's correction or Fisher's test was used. Considering the distribution of data, Pearson's and Spearman's correlation were used in correlation measurements.

Results

A total of 42 cases were included in the study; 40% of all cases were benign (17/42) (Figures 3 and 4) and 60% were malignant (25/42) (Figure 5). The mean age was 44.17 ± 7.56 in benign cases and 44.64 ± 11.32 in malignant cases, and no significant difference was found ($P > .05$). Although the most common mammographic microcalcification pattern in both groups was pleomorphic, it was significantly higher in the malignant group ($P = .037$). The most common contrast-enhancement kinetics with MRI in both benign

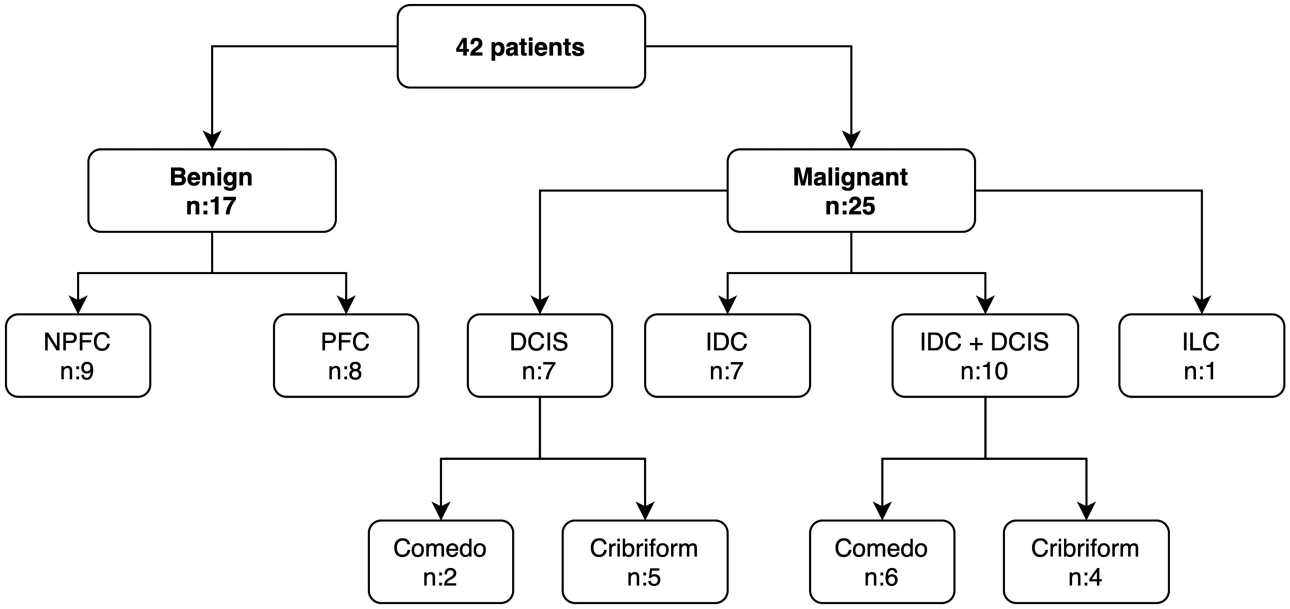

Figure 3. Flowchart summarizing the histopathological examination.
Abbreviations: NPFC, non-proliferative fibrocystic change; PFC, proliferative fibrocystic change; DCIS, ductal carcinoma in-situ; IDC: invasive ductal carcinoma; ILC, invasive lobular carcinoma.

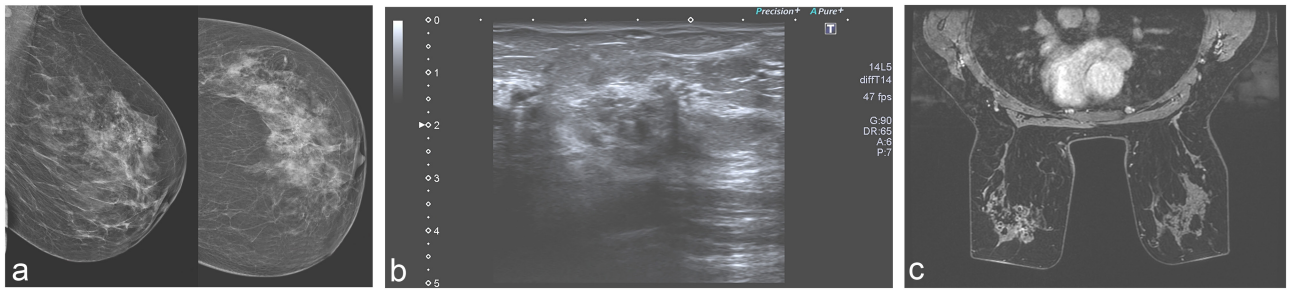

Figure 4. a-c. (a) In the mammographic examination of a 40-year-old female patient whose histopathology result was compatible with proliferative fibrocystic disease, coarse heterogeneous-amorphous calcifications were observed in a focal area of approximately 2 cm^2 in the upper outer quadrant of the left breast. (b) In the ultrasonographic examination, non-mass heterogeneous hypoechogenicity was observed in an area of approximately 2 cm^2 in the upper outer quadrant of the left breast in a localization suitable for this area. (c) On MRI, asymmetric, mild contrast enhancement was observed in an area of approximately 4 cm^2, in which T1W hypointense millimetric formations compatible with the cyst were observed. MRI, magnetic resonance imaging.

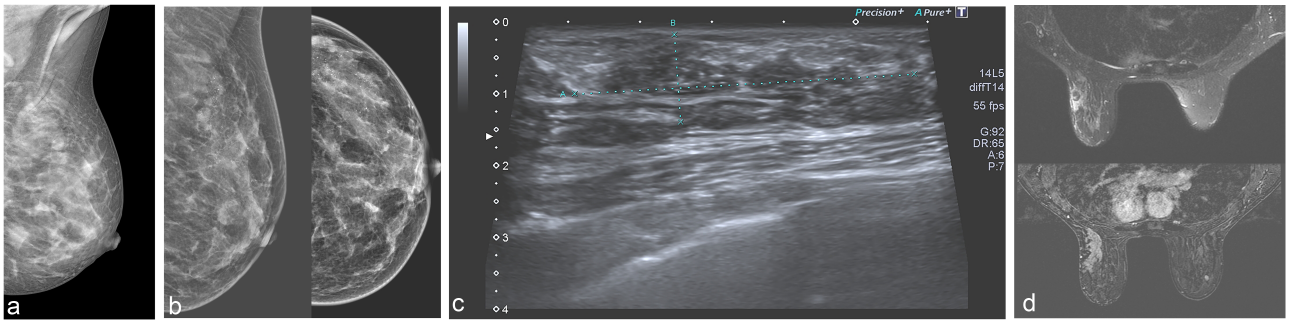

Figure 5. a-d. (a) Left breast MLO radiography dated 07.09.2017 of a 48-year-old female patient is seen. There was no feature in the dense breast parenchyma, except for benign nodular opacity with smooth contours in the upper part. (b) Mammographic examination dated 06.12.2019 of the case revealed newly developed pleomorphic microcalcifications suspicious for malignancy around this cyst, showing a segmental distribution in an area of approximately 5 cm^2. (c) In the sonographic examination, heterogeneity not accompanied by mass formation was noted in an area of approximately 5 cm^2 in the upper outer quadrant of the left breast in a localization compatible with this area. (d) In the MRI examination, asymmetric non-mass enhancements were observed in the breast parenchyma with respect to the right breast in a large area of approximately 7 cm^2, adjacent to the cyst in the upper outer quadrant of the left breast, and extending to the pectoral muscle in the posterior. Histopathological diagnosis by biopsy was reported as high-grade DCIS (grade 3). DCIS, ductal carcinoma in situ; MLO, mediolateral oblique; MRI, magnetic resonance imaging.

and malignant cases is type 2 pattern. It was seen in 47% of benign cases and 60% of malignant cases. The presence of axillary lymph nodes was significantly higher in the malignant group, but was not detected at all in the benign group (P = .013). The most common histopathological subtype in the malignant group was luminal A (56%), then Her2 (+) (32%) and luminal B (12%) (Table 2). In total, 28% (n = 7) of all malignant lesions are low grade (grade 1), 72% (n = 18) of them were high grade (grade 2-3), and 95% of high-grade lesions had an invasive component (17/18), whereas only 14% of low-grade lesions had invasive component (1/7).

Patients with microcalcifications that were not accompanied by a mass on MMG were included in the study. A non-mass enhancement pattern was observed in patients with MRI, too. No enhancement was detected with MRI in 3 of the patients; 2 of these were benign (non-proliferative fibrocystic change) and 1 was malignant (DCIS). Among 39 patients, the most common non-mass enhancement patterns was 41% (n = 16) focal; others were 26% (n = 10) regional, 26% (n = 10) linear, and 7% (n = 3) segmental contrast enhancement (Figure 2).

According to histopathological subtypes, the largest pathological area was seen in the invasive lobular carcinoma (ILC) (60 mm^2) and DCIS accompanying with IDC (IDC + DCIS) (46 mm^2). The largest areas in all lesions except ILC and IDC were detected by MRI. (Table 3). For benign lesions, the mean pathological area was 37.53 ± 21.71 mm^2 in MRI, 28.41 ± 9.79 mm^2 in MMG, and 23.23 ± 9.48 mm^2 in US (Table 3). For malignant lesions, the mean pathological area was 32.13 ± 19.22 mm^2 in MRI, 40.96 ± 22.63 mm^2 in MMG, and 27.48 ± 15.37 mm^2 in US (Table 3).

Although the sizes of malignant lesions on MRI and US were larger than benign ones, no significant difference was found (P > .05) (Table 4). There was a statistically significant moderate correlation between MMG and US in showing both benign and malignant lesions, but no correlation was observed with MRI (in benign lesions: P = 0.658, P = .004; in malignant lesions: P = 0.519, P = .008).

Discussion

Contrast-enhanced breast MRI is an imaging method based on immature neovascularization of tumor tissues.[6] They are diagnosed with the rapid staining of the immature vascular structures after injection of contrast agent and its leak-out into the extravascular area, which was named as the wash-out phenomenon.[6] Magnetic resonance imaging is a very sensitive method especially useful in the diagnosis of high-grade DCIS.[7] Rapid contrast enhancement or wash-out phenomenon may not be seen in low-grade DCIS because neovascularization is insufficient. This means that even if there is no pathological enhancement on MRI, there is a possibility of DCIS if there are suspicious findings on MMG and/or US. Therefore, low-grade DCIS can be diagnosed only by mammographic examination in the presence of calcification. On the contrary, in the diagnosis of DCIS that does not show calcification, false negativities can be seen in MMG.[6,7] Another important issue is that in the presence of invasive components, contrast enhancement tends to be more in the form of a mass in DCIS.[8] This explains why pathologically enhanced areas on MRI in malignant cases were smaller than those in MMG in our study. While there is contrast enhancement in a wider area in DCIS, enhancement can be seen in a smaller focal area only if there is an invasive component. The largest forehead size seen in ILC in this study can be explained by the spread of lobular carcinoma in a wider area than ductal carcinomas.

Non-mass enhancements on MRI are classified as focal, linear, segmental, regional, or diffuse in the ACR-BI-RADS MRI lexicon, just as stated in the MMG lexicon.[5,9] With MRI, the distribution of the tumor in the breast is determined with higher accuracy than MMG.[10-13] The presence of additional foci and the condition of the contralateral breast are also evaluated with MRI taken before the operation. This situation is very important in preoperative local staging and making the operation decision.[12-14] In our study, cases with suspected microcalcification in the category of BI-RADS 4-5 on MMG were evaluated by both US and MRI.

Table 2. General Features of Patients and Lesions According to Benign/Malignant Status

	Benign/Malignant		
	Benign	**Malignant**	***P***
Age (mean ± SD)	44.17 ± 7.56	44.64 ± 11.32	
Contrast-enhancement kinetics in MRI			.651
Type 1	6	4	
Type 2	10	13	
Type 3	1	5	
Diffusion restriction			.963
Yes	6	9	
No	11	16	
Morphology of mcc			**<.001**
A	7	4	
RH	2	6	
P	8	15	
Distribution of mcc			**.037**
R	8	8	
C	8	9	
L	-	1	
S	1	8	
Axillary involvement			**.013**
Yes	-	8	
No	17	17	
Molecular subtype			**<.001**
Her 2(+)	-	8	
Luminal A	-	14	
Luminal B	-	3	
Necrosis			**.002**
Yes	2	15	
No	15	10	
BI-RADS			**<.001**
4a	7	1	
4b	9	9	
4c	-	8	
5	1	7	

mcc, microcalcifications; A, amorphous; RH, rough heterogeneous; P, pleomorphic; R, regional; C, clumped; L, linear; S, segmental.

Table 3. Evaluation of Pathological Areas in MRI, US, and Mammography According to Histopathological Findings

		Pathological Areas (mm^2)			
	Number (n)	**Min**	**Max**	**Mean**	**SD**
IDC					
MRI	6	20.00	84.00	42.33	23.30
MMG	7	20.00	60.00	34.86	13.50
US	7	15.00	35.00	24.71	8.56
DCIS					
MRI	6	15.00	66.00	38.67	20.42
MMG	7	14.00	80.00	37.14	21.19
US	7	10.00	25.00	17.14	5.18
IDC+DCIS					
MRI	9	10.00	50.00	22.00	11.61
MMG	10	7.00	90.00	46.00	28.92
US	10	6.00	60.00	34.40	19.11
NPFCD					
MRI	7	15.00	83.00	42.29	23.29
MMG	9	15.00	50.00	28.22	11.11
US	9	14.00	50.00	24.22	11.12
PFCD					
MRI	8	10.00	64.00	33.38	20.85
MMG	8	16.00	45.00	28.63	8.83
US	8	14.00	32.00	22.13	7.85
ILC					
MRI	1	23.00	23.00	23.00	
MMG	1	60.00	60.00	60.00	
US	1	50.00	50.00	50.00	

MRI, magnetic resonance imaging; MMG, mammography; US, ultrasonography; DCIS, ductal carcinoma in situ; IDC, invasive ductal carcinoma; ILC, invasive lobular carcinoma; PFCD, proliferative fibrocystic disease; NPFCD, non-proliferative fibrocystic disease.

There was a moderate correlation between MMG and US dimensions.

DCIS, which are considered to be the precursor of invasive carcinomas, are usually asymptomatic and diagnosed with screening using MMG and may present as mass and non-mass enhancement on MRI.[10] Those seen as mass are usually accompanied by an invasive component.[7,11] In our study, in which non-mass enhancements in MRI were included, 72%

Table 4. Pathological Area Distribution According to MRI, Mammography, and US in Benign and Malignant Lesions

	Benign (n = 17)				Malignant (n = 25)				P*
	Mean ± SD (mm²)		Range (mm²)		Mean ± SD (mm²)		Range (mm²)		
	Mean	SD	Min	Max	Mean	SD	Min	Max	
MRI	37.53	21.71	10	83	32.13	19.22	10	84	.312
MMG	28.41	9.79	15	50	40.96	22.63	7	90	.192
US	23.23	9.48	14	50	27.48	15.37	6	60	.285

*Mann–Whitney U test; $P < .05$.

of malignant cases were high grade, and almost all of them had invasive components (17/18; 95%).

The relationship between the nuclear grade of DCIS and calcification has been shown in many studies up to now.[15,16] Necrosis as a result of malnutrition of fast-growing aggressive tumor cells gives an appearance as microcalcification on MMG, and this is most common in the high-grade comedo type.[1] Therefore, it is concluded that DCIS detected as microcalcification in MMG is higher grade. In our study, 60% of the BI-RADS 4-5 microcalcifications detected and biopsied were malignant microcalcifications and 72% of malignant microcalcifications were high grade, too. The type and distribution pattern of microcalcifications are also important in terms of malignancy predictivity and can change the BI-RADS classification and biopsy decision.[1,2]

Microcalcification evaluation by US is very difficult. Today, technological progress has been made in detecting mammographic microcalcifications with high-resolution low-frequency ultrasonographic devices.[9] However, even if microcalcifications are not seen by US, accompanying findings such as heterogeneous hypoechoic area, mass formation, parenchymal distortion, irregular ductal ectasia, microcyst cluster formed by obstructed ducts can be evaluated with US.[9] Despite all this, the ultrasonographic examination is still limited compared to other methods, especially in the diagnosis and prevalence of DCIS.

The major limitation of our single-center retrospective study is the small number of patients. The most important technical limitation is that lesions that could be seen by ultrasound underwent US-guided core biopsy, but those that could not be seen underwent excisional biopsy after the MMG-guided wire localization. This situation may cause many unnecessary surgical procedures of histopathological benign cases. Another limitation is that it is not known whether patients who underwent biopsy diagnosed with benign histopathology turn into malignancy in the future since we cannot follow patients for a long time.

As a result, MRI is the gold standard radiological method in breast imaging as well as in providing information about the real tumoral extension, additional focus and the condition of the contralateral breast, and in guiding the clinicians in terms of treatment and surgical procedure. It should be kept in mind that contrast enhancement may not be seen with MRI in low-grade or early-onset DCIS cases; therefore, in the presence of suspicious sonomammographic findings, even if MRI examination is negative, further histopathological evaluation should be performed.

Ethics Committee Approval: Ethics committee approval was received for this study from the ethics committee of Gaziosmanpaşa Training and Research Hospital (Date: April 14, 2021, Number: 252).

Informed Consent: Written informed consent was obtained from patients who participated in this study.

Peer-review: Externally peer-reviewed.

Author Contributions: Concept – D.E.T.Ş., Y.K., N.U.Y., A.N.Ş.; Design – D.E.T.Ş., Y.K., N.U.Y., A.N.Ş.; Supervision – D.E.T.Ş., A.N.Ş., N.U.Y.; Materials – Y.K., N.U.Y.; Data Collection and/or Processing – Y.K., N.U.Y.; Analysis and/or Interpretation – D.E.T.Ş., E.E., M.T.A., A.N.Ş.; Literature Search – D.E.T.Ş., E.E., M.T.A., A.N.Ş.; Writing Manuscript – D.E.T.Ş.; Critical Review – Y.K., N.U.Y., E.E., M.T.A., A.N.Ş.

Conflict of Interest: The authors have no conflicts of interest to declare.

Financial Disclosure: The authors declared that this study has received no financial support.

Etik Komite Onayı: Bu çalışma için etik komite onayı Gaziosmanpaşa Eğitim ve Araştırma Hastanesi'nden (Tarih: 14 Nisan 2021, Sayı: 252) alınmıştır.

Hasta Onamı: Yazılı hasta onamı bu çalışmaya katılan hastalardan alınmıştır.

Hakem Değerlendirmesi: Dış bağımsız.

Yazar Katkıları: Fikir – D.E.T.Ş., Y.K., N.U.Y., A.N.Ş.; Tasarım – D.E.T.Ş., Y.K., N.U.Y., A.N.Ş.; Denetleme – D.E.T.Ş., A.N.Ş., N.U.Y.; Malzemeler – Y.K., N.U.Y.; Veri Toplanması ve/veya İşlemesi – Y.K., N.U.Y.; Analiz ve/veya Yorum – D.E.T.Ş., E.E., M.T.A., A.N.Ş.; Literatür Taraması – D.E.T.Ş., E.E., M.T.A., A.N.Ş.; Yazıyı Yazan – D.E.T.Ş.; Eleştirel İnceleme – Y.K., N.U.Y., E.E., M.T.A., A.N.Ş.

Çıkar Çatışması: Yazarlar çıkar çatışması bildirmemişlerdir.

Finansal Destek: Yazarlar bu çalışma için finansal destek almadıklarını beyan etmişlerdir.

References

1. Fadare O, Clement NF, Ghofrani M. High and intermediate grade ductal carcinoma in-situ of the breast: a comparison of pathologic features in core biopsies and excisions and an evaluation of core biopsy features that may predict a close or positive margin in the excision. *Diagn Pathol*. 2009;4:26. [CrossRef]
2. Spak DA, Plaxco JS, Santiago L, Dryden MJ, Dogan BE. BI-RADS® fifth edition: a summary of changes. *Diagn Interv Imaging*. 2017;98(3):179-190. [CrossRef]
3. Ghaderi KF, Phillips J, Perry H, Lotfi P, Mehta TS. Contrast-enhanced mammography: current applications and future directions. *RadioGraphics*. 2019;39(7):1907-1920. [CrossRef]
4. Schell AM, Rosenkranz K, Lewis PJ. Role of breast MRI in the preoperative evaluation of patients with newly diagnosed breast cancer. *AJR Am J Roentgenol*. 2009;192(5):1438-1444. [CrossRef]
5. American College of Rheumatology Research and Education Foundation. *ACR BI-RADS® Atlas Fifth Edition*. Available at: https://www.acr.org/-/media/ACR/Files/RADS/BI-RADS/BIRADS-Reference-Card.pdf.
6. Newstead GM. MR imaging of ductal carcinoma in situ. *Magn Reson Imaging Clin N Am*. 2010;18(2):225-40, viii. [CrossRef]
7. Tajima CC, de Sousa LLC, Venys GL, et al. Magnetic resonance imaging of the breast: role in the evaluation of ductal carcinoma in situ. *Radiol Bras*. 2019;52(1):43-47. [CrossRef]
8. Lee KH, Han JW, Kim EY, et al. Predictive factors for the presence of invasive components in patients diagnosed with ductal carcinoma in situ based on preoperative biopsy. *BMC Cancer*. 2019;19(1):1201. [CrossRef]
9. Soo MS, Baker JA, Rosen EL. Sonographic detection and sonographically guided biopsy of breast microcalcifications. *AJR Am J Roentgenol*. 2003;180(4):941-948. [CrossRef]
10. Mossa-Basha M, Fundaro GM, Shah BA, Ali S, Pantelic MV. Ductal carcinoma in situ of the breast: MR imaging findings with histopathologic correlation. *RadioGraphics*. 2010;30(6):1673-1687. [CrossRef]. Erratum in: *RadioGraphics*. 2011;31:316.
11. Jansen SA, Newstead GM, Abe H, et al. Pure ductal carcinoma in situ: kinetic and morphologic MR characteristics compared with mammographic appearance and nuclear grade. *Radiology*. 2007;245(3):684-691. [CrossRef]
12. Gruber IV, Rueckert M, Kagan KO, et al. Measurement of tumour size with mammography, sonography and magnetic resonance imaging as compared to histological tumour size in primary breast cancer. *BMC Cancer*. 2013;13:328. [CrossRef]
13. Taskin F, Kalayci CB, Tuncbilek N, et al. The value of MRI contrast enhancement in biopsy decision of suspicious mammographic microcalcifications: a prospective multicenter study. *Eur Radiol*. 2021;31(3):1718-1726. [CrossRef]
14. França LKL, Bitencourt AGV, Paiva HLS, et al. Role of magnetic resonance imaging in the planning of breast cancer treatment strategies: comparison with conventional imaging techniques. *Radiol Bras*. 2017;50(2):76-81. [CrossRef]
15. Scott-Moncrieff A, Sullivan ME, Mendelson EB, Wang L. MR imaging appearance of noncalcified and calcified DCIS. *Breast J*. 2018;24(3):343-349. [CrossRef]
16. Kim JH, Ko ES, Kim DY, et al. Noncalcified ductal carcinoma in situ: imaging and histologic findings in 36 tumors. *J Ultrasound Med*. 2009;28(7):903-910. [CrossRef]